Analysis of data from the South China Sea Upper Slope Sand Dunes Acoustics Experiment

Ching-Sang Chiu and D. Benjamin Reeder
Department of Oceanography
Naval Postgraduate School
Monterey, CA 93943
Phone: (831) 656-3239 Fax: (831) 656-2712 email: chiu@nps.edu

Award Numbers: N0001415WX200224, N0001415WX00851,
N0001415WX00226, N0001415WX00853

LONG-TERM GOALS

Our long-term research goals are: (1) the characterization, understanding, and prediction of the statistics (mean, variance and coherence) of low-frequency acoustic signals and ambient noise in the littoral zone. The signal statistics are primarily influenced by the ocean variability and bottom properties. The noise statistics are influenced by atmospheric forcing and shipping in addition to the ocean and bottom variability; (2) the development and improvement of inverse techniques for measuring the dynamics and kinematics of meso- and finer-scale sound speed structure and ocean currents in coastal regions; (3) the understanding of three-dimensional sound propagation physics including horizontal refraction and azimuthal coupling and the quantification of the importance of these complex physics in the prediction of sound signals transmitted over highly variable littoral regions.

OBJECTIVES

Under the joint sponsorship of the US Office of Naval Research (ONR) and the Taiwan Ministry of Science and Technology (MOST), this multiyear, US-Taiwan collaborative field study was launched in 2012. Preceded by pilot cruises in 2012 and 2013 to obtain the necessary experimental design information, the intensive main experiment was carried out in June 2014. Specifically, the joint field study has the following overall scientific objectives:

- To characterize the time and space scales and the distribution of large submarine sand dunes on the upper slope.
- To study the impact of the sand dunes, and the combined impact of sand dunes and nonlinear internal waves, on sound propagation, in terms of phenomenology, including anisotropic propagation characteristics, and two-dimensional (2D) and three-dimensional (3D) focusing/defocusing scattering phenomena.
- To study the associated statistics (mean, variance and coherence) of sound signal propagation over the sand dunes and their dependence on range, frequency and orientation.
- To examine the hypothesis that the internal tide and large trans-basin NIWs are the generation mechanism of the dunes.

- To study how enhanced bottom roughness in the dune field affects transformation and energy dissipation of the NLIWs and tides as they shoal over the upper continental slope.

The first three objectives are to be accomplished by the PIs and their acoustician colleagues in a three-year (FY15-17) data-analysis effort entailing space-time signal processing, empirical and analytical data analyses, and 2D and 3D acoustics modeling.

APPROACH

All fieldwork for this project was carried out in collaboration and coordination with our long-time Taiwan colleagues, utilizing their Research Vessels (RVs), Ocean Researcher 1 (OR1), Ocean Researcher 2 (OR2), Ocean Researcher 3 (OR3) and Ocean Researcher 5 (OR5). Pilot cruises were successfully carried out on the OR2 in 2012, and the OR2 and OR5 in 2013. The multibeam echo sounder (MBES) survey data collected in 2013 were used to design the main acoustic propagation experiment that was conducted in June 2014 aboard the OR1, OR3 and OR5. The cruises were scheduled to occur during a spring and a neap cycle of the tides, during which the internal waves had maximum and minimum amplitudes, respectively. The multi-ship operations were designed to allow the observation of the distribution and variation in spatial scales of the sand dunes, and examine the associated impacts on the sound fields over the two cycles. It has been our hypothesis that the sound field and its statistics are primary controlled by the spatial scale and distribution of the sand dunes during the neap cycle, whereas they are controlled by a combination of the sand dunes and internal waves during the spring cycle.

Data processing and analysis of the main-experiment data have begun in FY15 and will continue in the following two years, FY16 and FY17. The comprehensive analysis entails time series analysis and modeling to characterize and elucidate: the associated ocean dynamical and sedimentation processes; the anticipated nonstationary statistics; as well as anisotropic, 2D and 3D focusing/defocusing phenomena in the measured sound field. The focus of the analysis will relate the observed statistics and phenomena to the scales and distribution of the sand dunes, with and without the coexistence of the nonlinear internal waves.

WORK COMPLETED

Work completed in FY15 include:

1. Calibrated all acoustic and oceanographic data collected during the 2014 main experiment, performed quality check, and documented the times, positions, sampling rates, record lengths, data types, quality, etc. in a technical report to facilitate subsequent data processing and analyses by various PIs of this joint project.

2. Coordinated and participated in a workshop hosted by our Taiwan collaborators in March to review data processing progress, discuss initial analysis results, outline scientific topics/papers to be accomplished, and identify lead investigators responsible for each topic in accordance of expertise and research interest.

3. Completed a data and modeling analysis of the tonal transmissions to the VLA from an autonomous mobile sound source (EMATT). The results on the measured and modeled

coherence time and transmission loss, TL, are discussed and compared in more details in the next section.

4. Checked the consistency of the geoacoustic model developed from data collected from the 2013 pilot experiment by comparing model calculations of TL based on this geoacoustic model to TL data measured in the 2014 main experiment.

5. Employed data recorded by receivers moored in close proximity to the moored (700-1,200 Hz) sweeper sound source, amplitude (AM) demodulation technique and a two-path model to attain the mean source level, SL, and its standard deviation as a function of frequency.

6. Completed the processing for TL (versus frequency, transmission time and location) from the moored source to all the receivers using the same AM demodulation technique to calculate sound pressure level (SPL), and then subtracting SPL from SL.

7. Performed an initial analysis of the data from a "Lowered Package", which consisted of a CTD frame outfitted with the following instrumentation: CTD, optical transmissometer, fluorimeter, camera and lights, upward- and downward-looking Lowered ADCP (LADCP) and two Nobska Development Corporation Modular Acoustic Velocity Sensors (MAVS-4) mounted 1 m apart. The LP observations indicate horizontal current speeds exceeded 100 cm/s and reached a maximum of 200 cm/s, while vertical currents were observed to reach 30 cm/s. The Shields parameter for this environment well exceeds 0.1, indicating that the ISW-induced currents are capable of turbulent suspension and transport of the available sediment.

8. Initiated a theoretical and numerical study of resonant interaction between acoustic propagating modes and subaquaeous bedforms as a function of bedform wavelength, acoustic frequency and bedform packet length.

RESULTS

One component of the experiment was the deployment of an Expendable Mobile Acoustic Training Target (EMATT) to obtain complementary TL measurements that are continuous in range. The EMATT was deployed from R/V OR5. It was programmed to maintain speed at 1.54 m/s and depth at 30 m and transmit continuously, every minute, a 58-s-long 1.25-kHz tone at a SL of 150 dB re 1 μPa followed by a 2-s-long 1.25-3 kHz timing/ranging FM signal. The programmed track (shown in Fig. 1) entailed first running a 4-km straight-line route from the northwest (315^o bearing) to the southeast (135^o bearing) of a moored vertical line array (VLA) of receivers, followed by a two and a half circular run counterclockwise around VLA before heading southeast to the deep basin. The processing for TL data requires first determining the coherence time of the received signal in the presence of source motion and environmental changes, and then applying the coherence time (i.e., optimal integration time) to derive statistically reliable signal mean square pressure estimates (SMSPE) using power spectral density (PSD) estimation techniques with adequate number of degrees of freedom (i.e., frequency smoothing). Frequency smoothing also accounts for the effects of Doppler and gradual amplitude changes on the estimate. We define that a measured signal time segment is coherent when the SMSPE suffers less than a 1-dB degradation, and that the SMSPE is

statistically reliable when its random standard error is less 10%. We showed in a simulation study that the coherence time is determined by the statistics of the phase fluctuations in the received signal. Amplitude fluctuations have no effects. The SMSPE suffers a degradation of less than 1 dB when more than 50% of the phase fluctuations (i.e., deviations from the linear trend) in the time segment are within half of a quadrant, i.e., 45^{o}, independent of whether the phase fluctuations have normal or uniform statistics.

Using a wide-angle parabolic equation (PE) propagation model, the coherence times based on the coherence criterion of phase fluctuations were modeled in collaboration with Prof. Chen and her student at National Taiwan University (NTU). The modeled signal coherence times as the EMATT travels in a 2-km circle are superimposed on the bathymetry in the top panel of Fig. 1, and the coherence times along the northwest to southeast straight-line path are shown in the bottom panel. The model input includes an average sound speed profile derived from the moored CTD data collected during the same period when the EMATT was transmitting, bathymetry from the 2013 MBES survey, and a geoacoustic model developed from inversion of the 2013 transmission data. Since only the bathymetry is varying in the model, the bathymetry gradients are expected to control the modeled coherence times. As the simulated source travels in a circle with constant radius, the coherence time would be shortened where the change in bathymetry with respect to bearing is significant, for example, when the transmission paths are oriented along or diagonally to the sharp sound dune crests as shown in the top panel of the Fig. 1. On the other hand, much longer modeled coherence times (> 60 s) are realized when the transmission paths are oriented orthogonal to the sand-dune crests, along the wider sand-dune troughs, and toward sectors of relatively flat bathymetry. When the source is moving in a straight-line path, the modeled coherence times, as seen in the lower panel of the figure, show decreased coherence times as the source and receiver are closing in to each other. This is due to the increased number of significant multipaths in shorter distances, resulting in more complex signal interference pattern that changes more rapidly in range.

The measured coherence times are displayed in Fig. 2. Measured coherence times were only estimated from data out to 20 s. Therefore, a data value of 20 s represents equal to or longer than 20 s. While the range of the EMATT was accurately provided by the timing signals, the bearing of the EMATT was only successfully estimated using other receivers (with locations denoted by white triangles in Fig. 1) based on the measured travel-time differences from the processed (pulse compression) timing signals. Those locations where the EMATT was successfully positioned indicate that after completion of the straight-line path, the EMATT could not maintain the 2-km-radius circles as programmed, rather it spiraled counter clockwise to the North-West in the strong currents. Only comparison to the modeled coherence time along the straight-line path is meaningful. The statistics between the modeled and measured coherence times along the straight-line path in the ranges out to 2 km are consistent. The measured mean coherence time minus a standard deviation (~ 8 s) was chosen to be the single, and conservative, optimal integration time for estimating TL from the data.

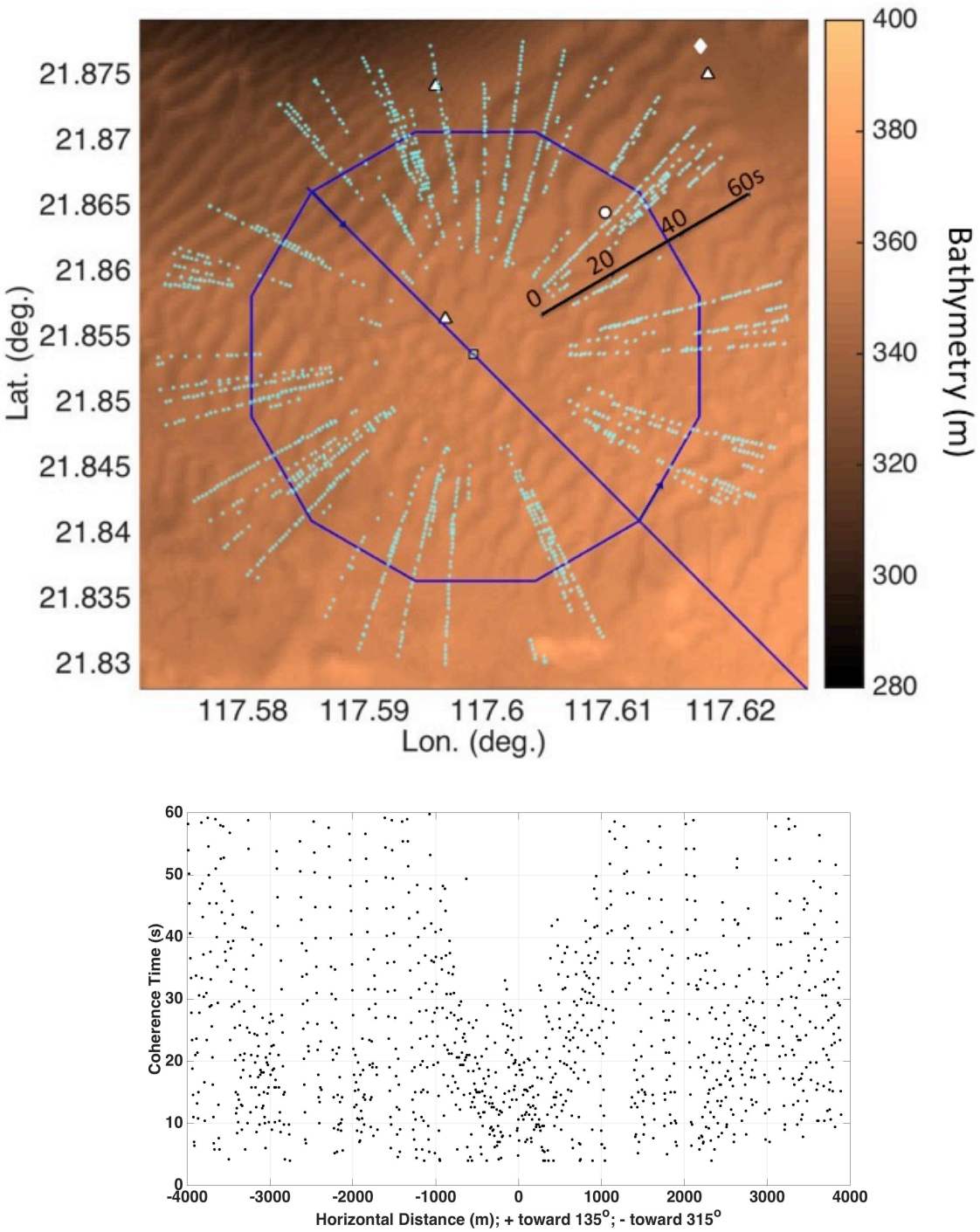

Fig. 1. Upper panel shows programmed EMATT track (blue) and modeled coherence time (light green dots) vs. bearing, for an EMATT transmitting a 1.25-kHz tone and moving along the circular path at a depth of 30 m and speed of 1.54 m/s, superimposed on the bathymetry mapped by a MBES survey. Lower panel shows modeled coherence time vs. range along the straight-line path at the same depth and speed. Receiver located at center of circle at a depth of 285 m.

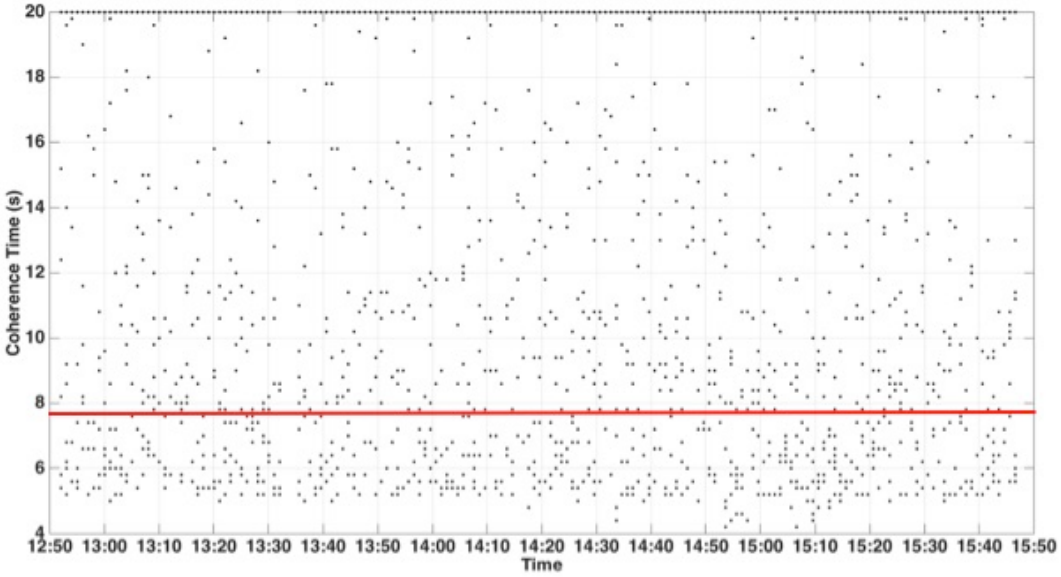

Fig. 2. Measured coherence time of a 1.25-kHz tone transmitted from an EMATT as a function of transmission time. Red line denotes the mean minus one standard deviation of the meausred coherence time.

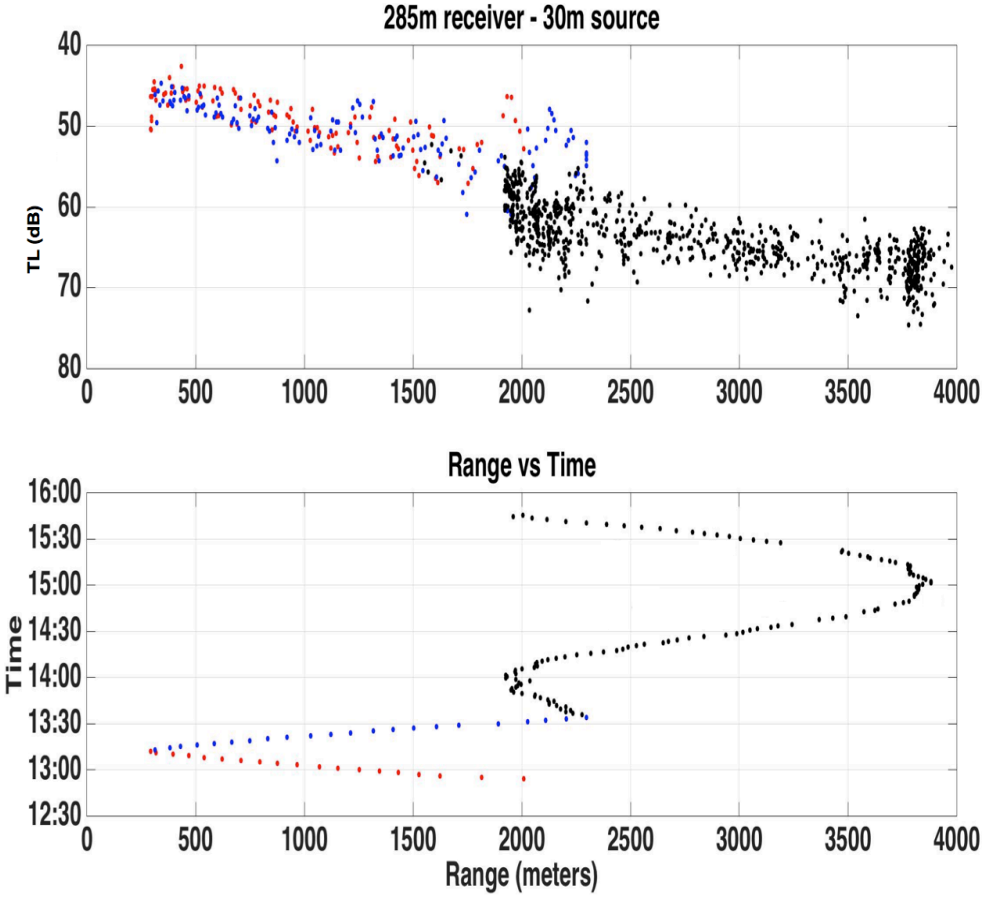

Fig. 3. Measured TL-versus-range for EMATT at 30-m depth and receiver at 285-m depth (top), and EMATT range vs. transmission time (bottom). Red dots denote EMATT on heading 135^o approaching the VLA, blue dots denote EMATT on heading 315^o leaving VLA, and black dots denote EMATT attempting the programmed circular track.

The resultant TL data are shown in Fig. 3, along with the corresponding ranging data. The range versus (transmission) time data, shown in the lower panel, clearly indicates that the initial straight-line path was well maintained. However, after completion of the straight path, the EMATT failed to maintain the programmed circular track, with a fixed radius of 2 km. The spacing between adjacent ranges contains curvature information. Larger spacing is indicative of no curvature (i.e., straight line), and smaller spacing indicates increased curvature.

In Fig. 4, both the modeled TL along a single radial and the measured TL are plotted together for a visual comparison. Note that the modeled TL displayed is for a bearing of 315^{o}, where as the TL data is on the same bearing up to 2 km, beyond which bearing information is lacking. Both the measured and modeled TL show two distinctive slopes, a steeper one corresponding to spherical spreading in ranges shorter than 2 km and a gentle slope beyond 2 km corresponding to cylindrical spreading in a low intensity zone. Near 2 km, both model and data show sound convergence structures. Measured and modeled TL are consistent with each other, more so in ranges shorter than 2 km but with increased discrepancies in ranges longer than 2 km where the actual bearings of the TL data are not known.

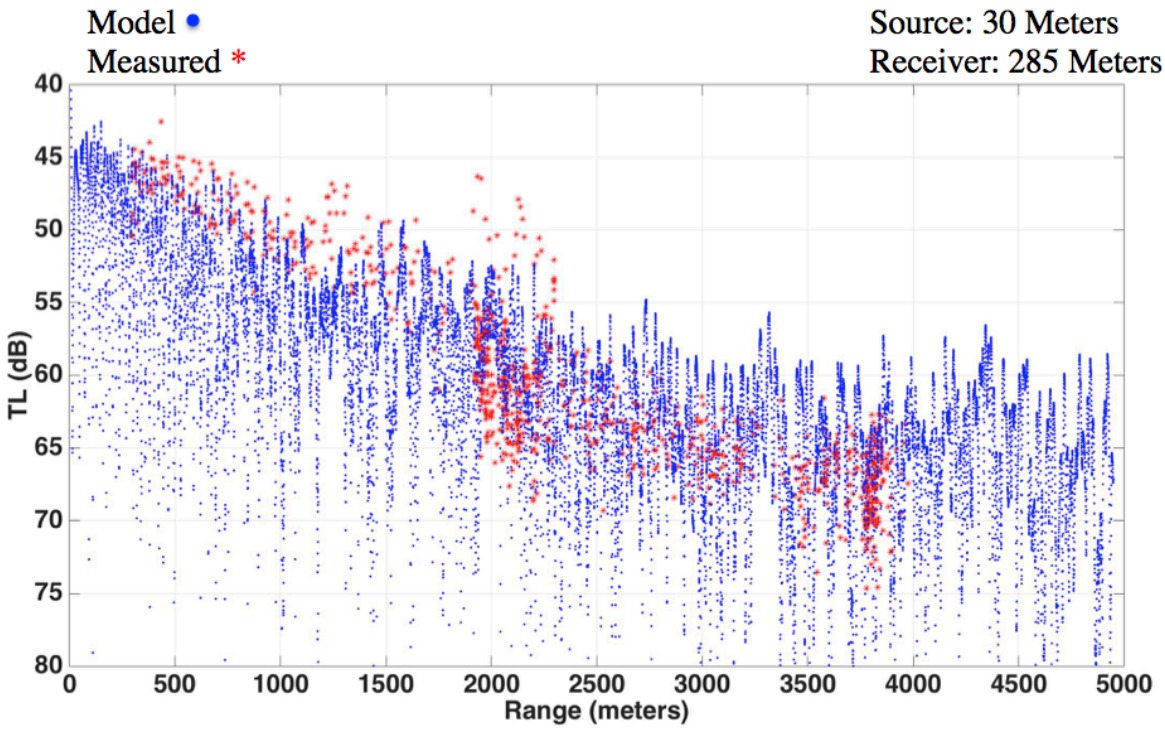

Fig. 4. Modeled TL along the 135° radial (blue) and measured TL (red), both at 1.25 kHz, as a function of horizontal distance from receiver. Source at 30-m depth and receiver at 285-m depth.

To check the consistency of the geoacoustic model developed from the 1.5-2 kHz and 4-5 kHz transmission data collect from the 2013 pilot experiment, we computed the resultant (i.e., predicted) TL from different sources to several receivers deployed during the 2014 main experiment. The modeling for the consistency check used the same geoacoustic model and MBES bathymetry, but with sound speed profiles obtained from the 2014 moored CTDs. The geoacoustic model has a layer of coarse sand with shells. The compressional speed, attenuation rate and thickness were estimated using least-squares estimation systematically searching in a volumetric grid for the minimum in the misfit function (often referred to as the ambiguity function). A 2-D slice of the misfit 3-D function at a thickness of 10 m is shown in left panel of Fig. 5, revealing that a best-fit compressional speed of 1750 m/s and a best-fit attenuation rate of 0.1 dB/m/kHz. The best-fit thickness estimate is larger than 7 m. The misfit function remains the same for thicknesses larger than 7 m. An example of the comparisons made between the predicted and measured TL in the 2014 main experiment for lower frequencies are shown on the left panel of Fig. 5. This example is for transmissions from a 600-Hz dipped source to three receivers at different depths on the VLA. Another example of consistency check is shown in Fig. 4 for a different frequency of 1.25 kHz. All these model-data comparisons suggest that revision of the geoacoustic model is not required.

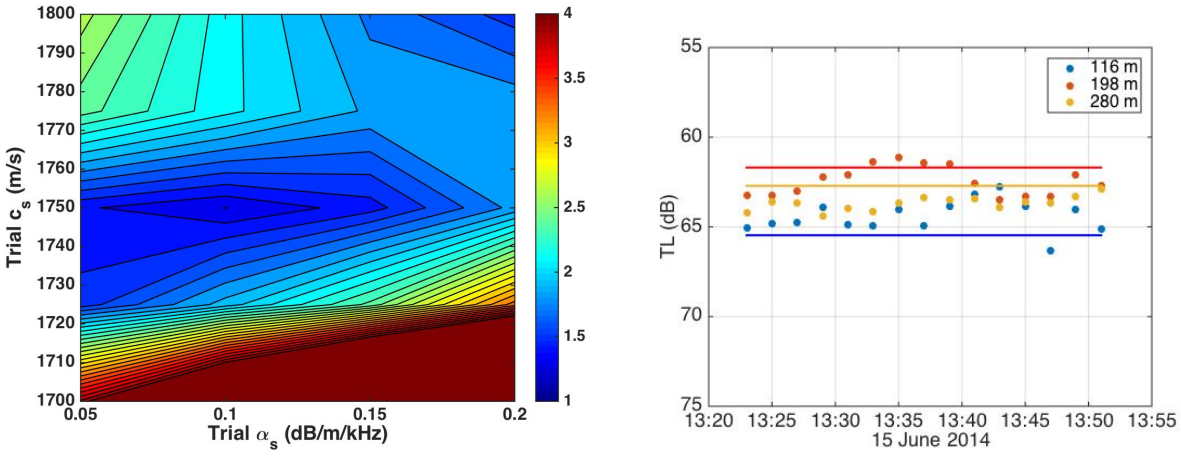

Fig. 5. Geoacoustic inversion result (left) based on least-squares fit to the 2013 pilot transmission data, showing a 2-D slice of the ambiguity (data misfit) function of three parameters: sand-dune compressional speed c_s, attenuation rate α and layer thickness. The slice shown is for a layer thickness of 10 m. Right panel shows the consistency of the predicted (lines) vs. measured (dots) TL at 600 Hz for three receiver depths at the VLA.

The processing for sound pressure level (SPL) as a function of frequency (from 700 to 1,200 Hz) and transmission time of the moored-source signal to all the receivers deployed in the 2014 main experiment has been completed. The processing used an amplitude (AM) demodulation technique to yield the instantaneous (in frequency or in time) squared pressure amplitude from all the time records of the signal. Note that frequency and time are related by the sweep rate of the source. Using the processed SPL data from four receivers in close proximity to the moored source, SL (i.e., SPL at 1 m from source) as a function of frequency was then estimated based on an analytical propagation model consisting of two paths, a direct path and a bottom-bounce path, each transmitting spherically spread sound pressure. The difference between the mean SL and the SPL measured at the different receiver locations at different transmission time then produced the measured frequency-dependent TL time series. The standard deviation of the SL provides an uncertainty estimate of the TL data.

The resultant mean SL and its standard deviation are shown in Fig. 6, whereas a resultant TL data time series is shown in Fig. 7. The TL time series displayed is for a receiver located near the VLA. Note that the SL dips in level near 775 Hz, but so does the SPL data at each receiver. This dip does not affect TL that is independent of SL and only depends on the environment. The measured TL changes expectedly, showing tidal patterns in time, and frequency selective patterns in frequency related to source and receiver depths. The second half (June 12 and beyond) had much bigger internal tides and waves that drove sound signal toward the bottom resulting in more scattering losses, thus higher TL (i.e., less intense). Also everyday as the internal tides and waves occupied and then left the transmission path, sound signal intensity went from a lower to a higher level for the same reason.

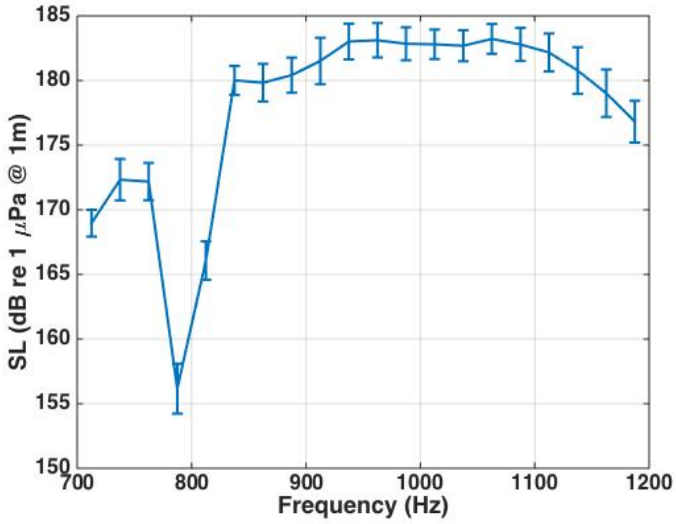

Fig. 6. Mean and standard deviation of the SL of the moored source, estimated from data obtained from a receiver array moored at a distance of 50 m from the source .

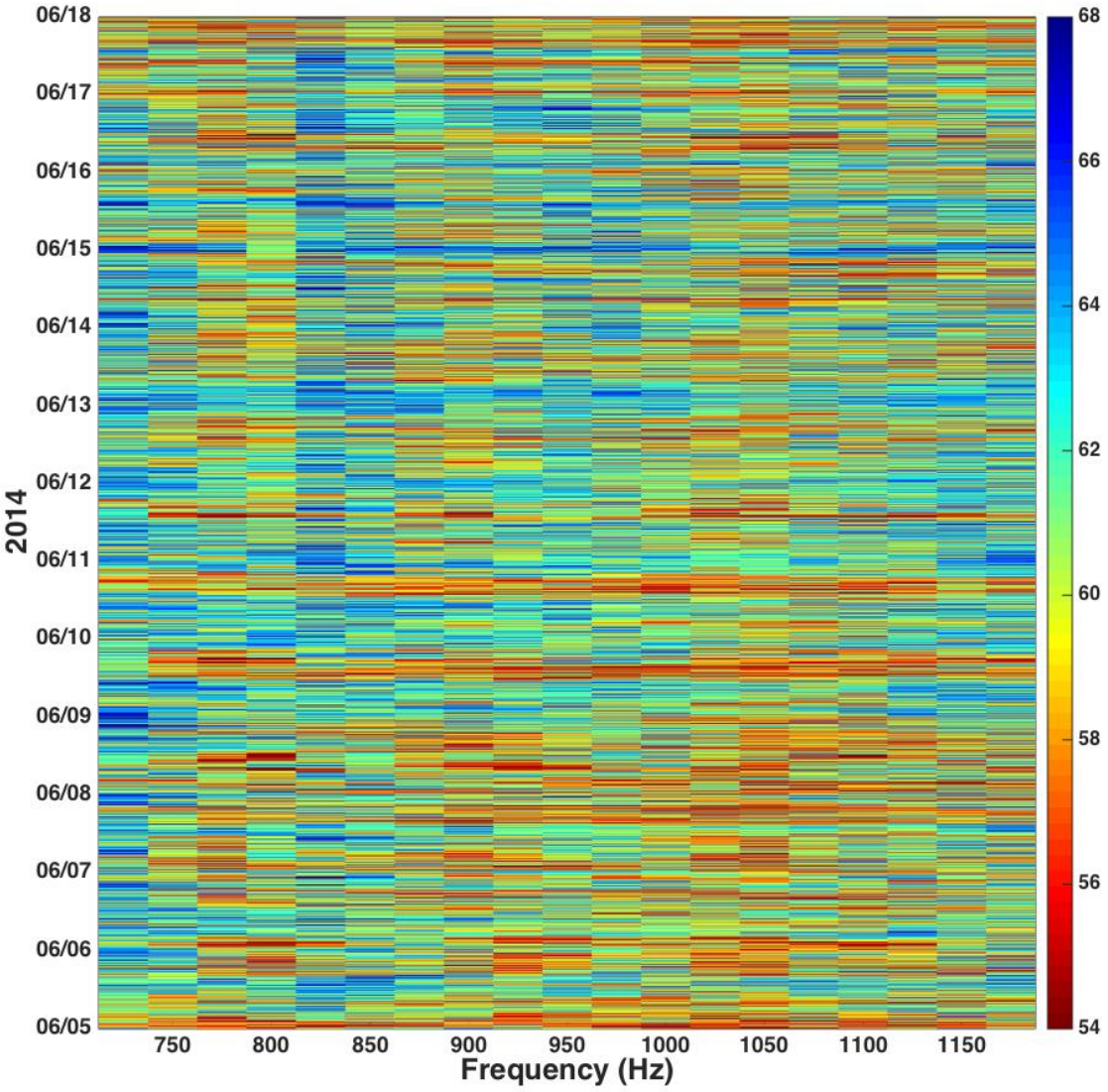

Fig. 7. Measured TL as a function of frequency and transmission time at a receiver located 3.2 km away from the moored source at a depth of 220 m.

IMPACT/APPLICATIONS

This study will contribute to the foundational scientific knowledge required to improve naval sonar system performance based on an understanding of the phenomenology and statistics of acoustic propagation in an environment having both sand dunes and ISW's. The dunes' location on the continental slope has profound implications on both active (i.e. increased reverberation from the continental slope for a surface ship operating in deeper water) and passive sonar (i.e. up/downslope propagation anomalies, angular dependencies, 3D effects, combined effects of the sand dunes and ISW's).

RELATED PROJECTS

This integrated acoustics, oceanography and geology experiment should extend the findings and data from SWARM, Shelfbreak PRIMER, ASIAEX, SW06 and NLIWI, thus improving our knowledge of the physics, variability, geographical dependence and predictability of sound propagation in a shelf-slope environment.

PUBLICATIONS

Miller, C.W., C.-S. Chiu, D.B. Reeder, Y.-J. Yang, L. Chiu and C.-F. Chen, "Preliminary Observations from the 2014 Sand Dunes Experiment," Naval Postgraduate School Technical Report NPS-OC-14-004, October 2015.

Graessle. S.W., "Measurement of transmission loss using an inexpensive mobile source on the upper slope of the South China Sea," Naval Postgraduate School MS thesis, September 2015.

Chang, A., L. Chiu and D.B. Reeder, "Resonant interaction of acoustic waves with subaqueous bedforms: Sand dunes in the South China Sea," *J. Acoust. Soc. Am.*. (submitted)

Reeder, D.B. and Y.-J. Yang, "Observations of near-seabed currents induced by very large internal solitary waves over a sand dune field in the South China Sea," *IEEE Proceedings of the Current, Waves and Turbulence Workshop*, St. Petersburg, FL, March 2015.